JOURNAL OF SPACECRAFT AND ROCKETS
Vol. 43, No. 3, May–June 2006

Degradation Testing of Spacecraft Materials for Long Flights in Low Earth Orbit

L. S. Novikov* and V. N. Chernik†
Moscow State University, 119992, Moscow, Russia
S. F. Naumov,‡ S. P. Sokolova,§ T. I. Gerasimova,¶ and A. O. Kurilyonok¶
Korolev Rocket and Space Corporation, 141070, Korolev, Russia
and
T. N. Smirnova**
Khrunichev State Space Scientific Production Center, 121087, Moscow, Russia

Results of simulation tests of the influence of the protective and functional coatings on the resistance of polymeric constructional spacecraft materials to the impact of atomic oxygen with fluences up to 3.5×10^{22} cm^{-2} are presented. It was demonstrated that oxygen plasma beams can be used in accelerated tests of carbon-based and polymeric material structures (with the exception of filled and fluorinated hydrocarbons) to evaluate their resistance to the atomic oxygen impact in low Earth orbit. For unprotected materials, a sharp fall of mechanical properties and a deterioration of optical characteristics were observed. The application of protective coatings is shown to reduce this degradation.

Nomenclature

dF	=	fluence increment
dM	=	mass loss
E	=	atomic oxygen translation energy
f	=	normalized energy dependence
K	=	Kapton® index
M	=	material index
Y	=	erosion yield
γ	=	protection efficiency

I. Introduction

ONE of the principal damaging factors of the space environment in low Earth orbit (LEO) is atomic oxygen (AO). In prolonged exposures of materials on the outside surfaces of spacecraft, their resistance to AO attack is of major importance. Because polymer-based materials are widely used on spacecraft and most of them are susceptible to AO attack, their protection by various means, including protective coatings, is necessary.

Many spacecraft surface structures are made from an assembly of different materials. Examples of such structures include textile parts of cases and screens lap-jointed together by spun thread seams, multilayer insulation fastening, cable braid, and fixation arrangements by thread, cords, ropes, etc. Although the AO resistances of many component materials are known, the actual behavior of assemblies needs to be tested under high-AO fluences.

Long-term LEO flight simulation requires irradiation of materials with AO fluences up to 10^{22}–10^{23} cm^{-2}. Simulator beam intensities do not exceed 10^{17} cm$^{-2} \cdot$ s^{-1} (usually 10^{15}–10^{16} cm$^{-2} \cdot$ s^{-1}) (Ref. 1), and this results in unacceptable test durations. The reduction of the test duration is achieved by increasing the particle beam energy within the limits of conservation of the interaction mechanism with the test material.[2]

In our work, the accelerated simulation material tests were carried out in oxygen plasma beams, formed by a plasma accelerator, with the AO species energy 20 eV. The changes of weight and mechanical and optical properties of materials and structures were investigated at equivalent AO fluences up to 3.5×10^{22} cm^{-2}.

II. Test Materials

Materials used for various purposes were investigated: structural coatings (black reinforced plastics, fabric, threads, films) and functional coatings (protective, thermocontrol, colored).

The black reinforced plastic is composed of carbon fibers and an epoxy matrix. Samples in the form of plates 1 mm thick without coating and with thermal control coating (TCC) white conductive enamel EKOM-1 were tested. The enamel EKOM-1 consists of ZnO pigment with acrylic binder, 0.1 mm thick.

An additional test object was a fragment of a folding shield designed to protect external International Space Station equipment from the impact of the space shuttle jets. The shield consists of Terlon fabric (Kevlar®-type polyamide) with separate parts overcast by the polyimide spun threads.

Another synthetic fibrous material was a sennit PARML. It is a conductive fibrous material applied to cable shielding. It is twisted with polyimide-fiber bundles that are the sennit load-bearing basis. Several bundles are wound around by copper tinsel ribbon for high electroconductivity.

Tensile, stress–strain measurements were used to evaluate the changes in the breaking load of the polyimide fibers threads, Terlon fabric, and sennit PARML.

To determine the efficiency of several protective coatings, polyimide films of 20- and 40-μm thickness were tested. The films were coated with silica layers of 0.2–0.4-μm thickness by means of sputter deposition. Other kinds of protection were silicone layers of 10–20-μm thickness. The layers were covered by spraying varnishes of two types. The first, silicone 3, was based on a linear silicone

Presented as Paper 2004-4 at the 7th International Conference on Protection of Materials and Structures from Space Environment, Toronto, ON, Canada, 10–13 May 2004; received 24 January 2005; revision received 1 September 2005; accepted for publication 10 September 2005.

*Head of Department, Department of Nuclear and Space Research, Skobeltsyn Institute of Nuclear Physics.
†Senior Staff Scientist, Department of Nuclear and Space Research, Skobeltsyn Institute of Nuclear Physics.
‡Principal Staff Scientist, Department of Material Engineering, 4a, Lenin St.
§Principal Engineer, Department of Material Engineering, 4a, Lenin St.
¶Engineer, Department of Material Engineering, 4a, Lenin St.
**Senior Staff Scientist, Department of Spacecraft Materials, 18, Novozavodskaya St.

polymer with polymethylsilasan as hardener. The second, silicone 5, was a polymethylvinylhidrosiloxan in toluene as a solvent.

We also tested color enamels with epoxy and silicone binders. Also we studied the efficiency of the epoxy enamels protection by a silicone varnish layer. The red, dark blue, white, black, and yellow coatings were applied to fiberglass fabric samples 20×40 mm in size.

III. Test Technique

In our work, the accelerated materials tests were carried out in oxygen plasma beams with an average energy of oxygen atomic species of 20 eV.

The plasma beam source is a magnetoplasmadynamic accelerator type, adopted to oxygen gas operation.[3,4] The source diagram is shown in Fig. 1. The dc arc oxygen plasma is accelerated by a self-consistent electrical field arising from the plasma expanding to a vacuum in the divergent solenoid magnetic field. A double plasma contraction is applied as in a duoplasmatron to reduce the beam contamination resulting from electrode erosion product emission. In this way, the beam impurity is as low as 3.5 Fe atoms per 10^6 oxygen ions.

The plasma source is operable in three modes with various oxygen species translation energy spectra: 5–15, 10–40, and 150–250 eV.

The simulation facility comprises two stainless-steel vacuum chambers, including a 400-mm cross source chamber housing the plasma accelerator assembly, connected to a 250-mm cross sample chamber. Differential pumping maintains a working vacuum of $0.5–2 \times 10^{-2}$ Pa by polyphenyl diffusion pumps with liquid nitrogen cooled traps.[3]

The plasma beam diagnostics is accomplished by plasma electric probes (ion flux), electrostatic energy analyzer (ion energy distribution), and monopolar mass spectrometer. Flux and average velocity of neutrals are evaluated by means of a bolometer/torsion balance device.[4] The beam impurity level of 3.5×10^{-6} Fe atoms per O atom is measured by means of a deposition probe with postexposure Rutherford backscattering analysis (see Ref. 4). During AO exposure, we evaluated the AO equivalent (effective) fluence (EF) using the witness polyimide film mass loss. The EF is not an absolute measure of AO projectiles arriving at the surface, but it is the calculation of the fluence of a fictitious 5-eV AO beam that would initiate the same polyimide mass loss as observed in the facility.[2] The EF is used usually as a means of comparison of LEO AO impact with simulative ground-based effects when the AO energy is less[5] or higher[2] than 5 eV. The EF was calculated on the assumption of a polyimide erosion yield $Y = 4.4 \times 10^{-24}$ g/atom O under LEO impact.

To increase the erosion yield and, hence, to accelerate the testing, we used a mode of source operation when the beam was a mix of oxygen atoms, molecules, and ions with an average velocity raised up to 13–16 km/s (mean atom energy of 20 eV) and a beam flux density of $0.5–1.5 \times 10^{16}$ cm$^{-2} \cdot$ c^{-1}. The latter corresponds to an effective LEO AO flux of $3.5–7.5 \times 10^{16}$ cm$^{-2} \cdot$ c^{-1}, based on a Kapton® equivalent. Only atoms with an average velocity of 13–16 km/s are supposed to react with the material due to the dissociation of fast molecules and ion neutralization on collision with surface.

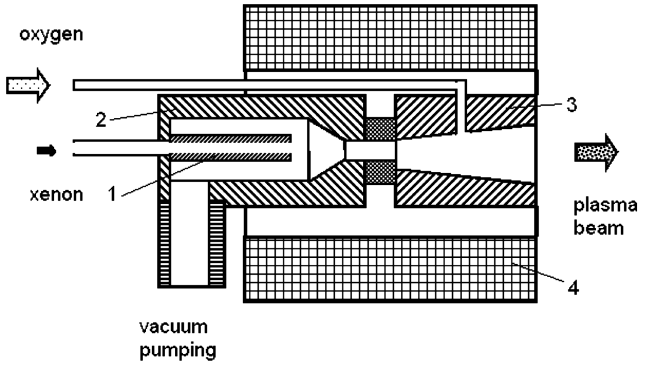

Fig. 1 Oxygen plasma source diagram: 1, hollow cathode; 2, ferromagnetic intermediate electrode; 3, anode; and 4, solenoid.

Because the experimental conditions are different from LEO we interpreted the test data as follows. We presented a material erosion yield Y_M as a function of energy E (electron volts), that is,

$$Y_M(E) = Y_M(5) \times f_M(E)$$

where $f_M(E)$ is a normalized energy dependence, $f_M(E) = 1$ if $E = 5$ eV.

Actually by means of the Kapton equivalent, we evaluate a relative erosion yield Y_M/Y_K of the material tested with regard to Kapton Y_K but not the absolute one. In this way the desired result is

$$\frac{Y_M(5)}{Y_K(5)} = \frac{Y_M(E)/f_M(E)}{Y_K(E)/f_K(E)} = \frac{Y_M(E)}{Y_K(E)} \times \frac{f_K(E)}{f_M(E)}$$

$$= \frac{\mathrm{d}M_M(E)}{\mathrm{d}M_K(E)} \times \frac{f_K(E)}{f_M(E)}$$

This imples that the erosion yield measured at 20 eV distinguishes from the LEO one by factor of $f_K(20)/f_M(20)$.

There is a good reason to think the factor is close to unity for many nonfluorinated unfilled polymers and carbon. The materials undergo oxidative erosion on the pathways of H abstraction and elimination, O addition and insertion, and C–C bond breakage.[6] However, all branches of oxygen interaction pathways eventually lead to volatile lower oxides. The reaction thresholds lie below 5 eV. As AO energy rises above 5 eV, the reaction cross section grows and erosion yield increases,[7] but the oxidative erosion mechanism remains the primary channel of mass loss up to the sputtering threshold. The sputtering fraction in mass loss of Kapton is smaller by at least one order of magnitude at an AO energy 30 eV (Ref. 8). Hence, in this energy range, the erosion yields of hydrocarbon polymers appear to increase as a universal oxidation-dependent energy function.

The assumption is confirmed experimentally. It has been shown at the Physical Sciences, Inc. (PSI), laser pulsed fast atom source that erosion yields of polyimide, polyethylene, and graphite vary as translation energy squared in the obtainable range up to 16 eV (Ref. 9).

The erosion yield of an unprotected black reinforced plastic, measured in our tests, was 1.7×10^{-24} g/O atom. It corresponds to ground-based results (1.8×10^{-24} g/O atom) on a Toulouse Research Center (CERT–ONERA) simulator under a 5-eV AO beam[10] and is close to the long duration exposure facility flight data (1.6×10^{-24} g/O atom) (Ref. 11).

The pure epoxide erosion yield measured in our facility was 2.2×10^{-24} g/O atom vs 2.1×10^{-24} g/O atom in LEO.[11]

The results indicate the plasma accelerator conditions to imitate adequately the LEO mass loss of the polymers and carbon-based materials with the AO fluence measured by means of the Kapton equivalent. We suppose that this conclusion may be extended to many unfilled nonfluorinated polymers.

When material properties were studied, the changes of weight and thickness were measured, and the reflection spectra in the range 0.2–2.5 μm were registered. The stress–strain properties were determined on a tensile test machine.

IV. Experimental Results

A. Protection Efficiency of TCC White Enamel Coating of Black Reinforced Plastic

The specific mass loss and thickness of the black reinforced plastic samples uncoated and coated by EKOM-1 as a function of the AO EF are given in Fig. 2. The exposure was to an oxygen plasma beam with AO energy of 20 eV. We tested identical samples when measuring their mass losses and thicknesses. As can be seen, thicknesses of the uncoated samples are linear functions of the AO fluence. At the same time, the mass loss of the coated sample is lower by a factor of 6.5, and the thickness change is negligibly small. On the mass loss curve of the bare sample, we observe the change in slope at approximately 9×10^{21} cm^{-2}. At the initial part, with a pure epoxy layer etching, the yield is 2.2×10^{-24} g/O atom. It corresponds to yield of an epoxide in LEO, 2.1×10^{-24} g/O atom. When the epoxy layer on the surface has been removed, carbon fibers become naked. The yield decreases to 1.8×10^{-24} g/O atom in accordance with

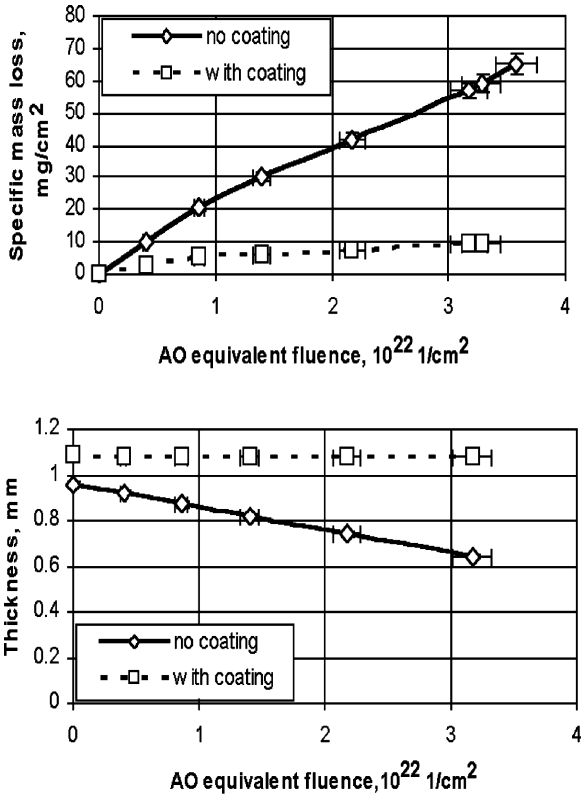

Fig. 2 Specific mass loss and thickness of samples of black reinforced plastic uncoated and with EKOM-1 enamel coating as functions of AO equivalent fluence.

LEO yield of a black reinforced plastic, 1.6×10^{-24} g/O atom. Close results were obtained at a CERT–ONERA pulsed laser detonation facility at an AO beam energy of 5 eV (Ref. 10). For an initial etching period, the yield was 2.6×10^{-24} g/O atom, then under greater AO fluences, it decreased to 1.8×10^{-24} g/O atom.

Scanning electron microscopy of samples exposed showed the polymer binder on the bare samples to be etched away and fibers to be partially destroyed. As a result, the surface roughness increased.[12]

The picture was similar to observations made during in-flight experiments onboard the space shuttle spacecraft, Salute-6, and Mir space stations.

B. Degradation of Mechanical Properties of Synthetic Fiber Materials

The results of measurements of specific mass loss of the Terlon fabric samples and the sennit PARML samples show that the Terlon fabric is close to polyimide in AO resistivity because the materials mass losses are close to 5.4 and 5.6 mg/cm^2, respectively.

A complete etching of the polyimide fibers in a significant part of the bundles in the sennit PARML was observed. To ascertain the influence of the exposure on strength properties, we carried out a comparison mechanical test of the exposed sample and a reference sample. According to Russian State Standard (GOST 3813-72), on textile material mechanical tests one must measure a breaking load and elongation at rupture of textile and fibrous materials. We tested three exposed and five reference samples of each kind of material.

The characteristic tensile stress–strain diagrams of the sennit PARML samples (reference and exposed to AO EF of 3.7×10^{21} cm^{-2}) are given in Fig. 3. The exposure was to an oxygen plasma beam at AO energy of 20 eV. The ultimate load reduction by a factor of five and the increase of relative elongation at fixed load of 200 N by a factor of seven demonstrated the drastic collapse of strength properties.

After AO exposure, the destruction of seam threads and Terlon fabric was observed on the fragment of the shield. The fragment consists of two Terlon fabric tapes lap jointed by a polyimide thread seam. The sample dimensions are width 20 mm, thickness 0.5 mm,

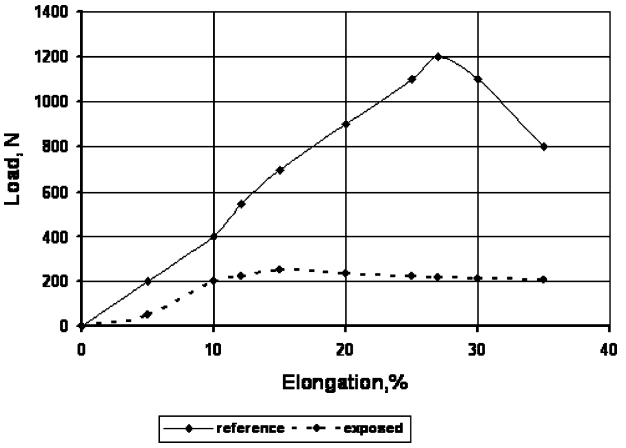

Fig. 3 Tensile stress–strain of sennit PARML reference and exposed samples.

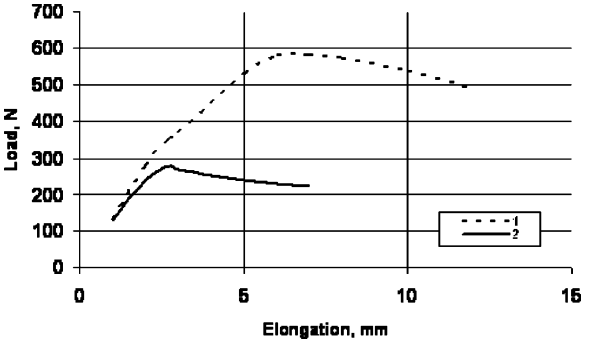

Fig. 4 Tensile stress–strain diagrams of - - -, reference and ——, AO exposed samples of shield fragments.

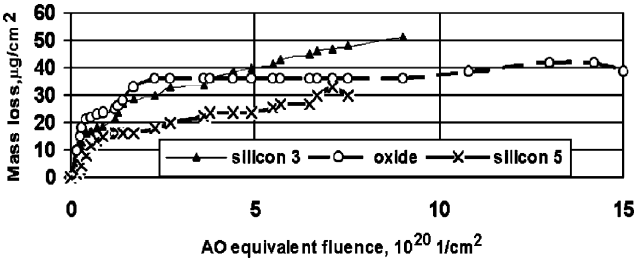

Fig. 5 AO fluence dependences of the mass loss of the polyimide films with protection by silica layers deposited and silicone coatings of silicone 3 and silicone 5.

and gauge length 40 mm. The characteristic tensile stress–strain diagrams of the reference and AO exposed samples of the shield fragments are presented in Fig. 4. Here, the exposure was to an oxygen plasma beam with an AO EF of 8×10^{21} cm^{-2} at energy of 20 eV. When loading up to approximately 20-fold working load, identical elongations were observed in both samples. By further increasing the loading, the exposed sample failure manifests itself as a sharp break in the curve and an increase in elongation is observed without an increase in or even with reduction of loading. The elongation on rupture of the exposed sample also decreases by a factor of 2.

C. Efficiency of Protective Silicon-Based Coatings

AO plasma treatment caused crazing of the silicalike layers. The crack net density was growing as flux or fluence increasing. The crack net form and density follow the film pincher form due to the sample clamping in a holder.

The mass loss dependences on the AO EF are shown in Fig. 5. The data represent the polyimide films protected by deposited silica layers and by silicone coatings of two varnish types. One can see

two parts on each curve. At the beginning of the exposure of AO energy of 20 eV, the slope is high due to samples outgasing, and then the comparatively flat part is observed.

On the latter, we define the AO protection efficiency γ as the bare film mass loss dM_K divided by the protected film loss dM_M under equal EF increment dF, that is,

$$\gamma = \left.\frac{dM_K}{dM_M}\right|_{dF=\text{const}}$$

The protection efficiency is greatest for the silica layer ($\gamma = 830$) and decreases up to $\gamma = 250$–430 for varnish coverings.[13] Though microcracks are generated, the silica layer protection ability stays high. We have not seen any etching marks usually observed under protection defects by optical microscopy. On the contrary, we observed no cracking in the silicone coatings. Nevertheless, the silicone protection efficiency is less then silica protection efficiency. The mass loss is assumed to originate from methyl group reactions with AO diffusing in the thick silicone layer through the thin protective barrier.

Thermooptical characteristics of the samples changed very little. For the silica coating, an insignificant reflectance reduction (uniform in wavelength) is observed that can be associated with scattering action of the microcrack grid. Thus, the solar absorptance grows from 0.366 to 0.380. The reflectance increase is typical for varnish coatings, especially appreciable in the long wavelength part of the spectrum.

The AO protection silica coating polyimide films were exposed on the Mir Space Station.[13] The material samples were installed on removable cassete-container returned to Earth after the LEO exposition. The mass losses varied in the range of 11–60 $\mu g \cdot cm^{-2}$ at fluences of 0.3–1.2 10^{21} cm^{-2}. The results are in agreement with our ground-based data.

D. Testing the Resistance of Color Paints

The paint test results have shown different AO resistance for various types of enamel.[14] The epoxy enamels coloring change and significant mass losses are observed. Dark blue and red enamels are almost completely bleached save only hint of their initial color. The black enamel becomes light-colored and gains a brown shade.

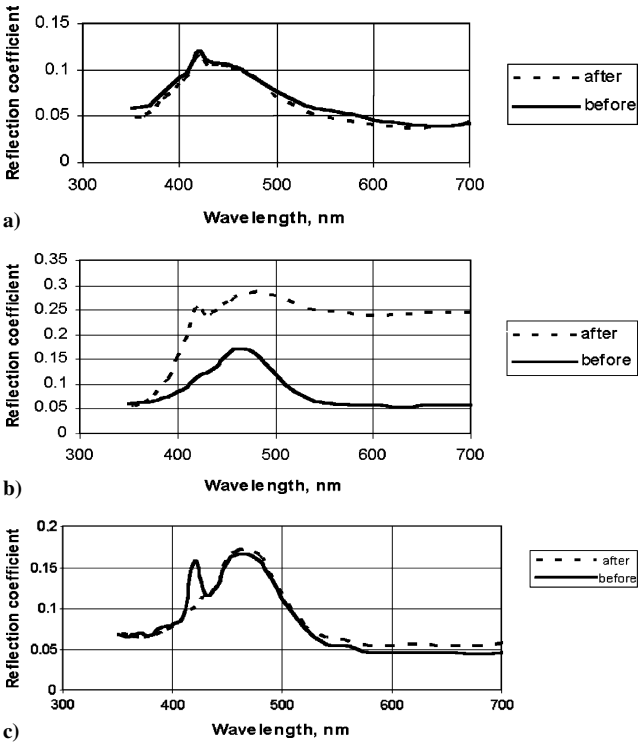

Fig. 6 Reflection spectra of dark blue paints in the visible wavelength range for three coatings: a) silicon KO-811K, b) epoxy EP-140, and c) epoxy EP-140 with silicone varnish coating KO-008, recorded before and after oxygen plasma beam exposure with AO equivalent fluence of 1.4×10^{21} cm^{-2} at energy of 20 eV.

The erosion yields of the color epoxy enamels (0.3–0.5×10^{-24} g/atom O) are much lower than that of the binder and of the witness polymers (3–4.4×10^{-24} g/atom O) and is explained by the protective action of the pigments.

The impact of oxygen plasma on silicone enamels almost does not change their color and mass.

Protection of the epoxy enamel by a silicone varnish layer increases the coating resistance up to the level of the silicone enamels. The erosion yields of these coatings are less than of the witness film by two orders of magnitude. Figure 6 shows the reflection spectra of the dark blue paints in the visible wavelength range for three coatings: epoxy EP-140, silicon KO-811K, and epoxy EP-140 with silicone varnish coating KO-008.

We can see on all initial spectra blue wave peaks. The silicone paint looks darker and demonstrates a lower reflectivity peak. In the epoxy postexposition spectrum, the blue wave peak disappears and a reflectivity increases uniformly all over the visible waveband. The effect is observed visually as color fading. On the contrary, silicone coatings retain their initial spectra.

When the spectra are compared, it is evident that the dark blue color peak seen in all initial spectra almost completely disappears for the epoxy enamel that is accompanied by an increase of reflectance in the whole range. Coloring and the spectra of other dark blue paints practically do not vary.

V. Conclusions

We used oxygen plasma beams created by means of the magnetoplasmadynamic accelerator to simulate the AO LEO impact on spacecraft materials and structures. Although the AO energy was greater (20 eV), we observed the erosion yield of the epoxy and carbon-based materials to be close to that at 5 eV if the AO effective fluence is measured by means of the Kapton equivalent. On the basis of the results and known data, we extend the conclusion to hydrocarbon polymers in the 5–20 eV AO energy range where a sputtering is negligible.

In that way, we demonstrated that oxygen plasma beams can be used in accelerated tests of carbon-based and polymeric material structures (with the exception of filled and fluorinated hydrocarbons) and protective coatings to evaluate their resistance to the AO impact during the simulation of the long flights in LEO.

The resistance of prospective spacecraft materials and structures, polyimide films, synthetic Terlon fabric, sennit PARML, black reinforced plastic, polymeric paints, and TCCs under oxygen plasma beams simulating the AO fluxes in LEO was investigated. For the unprotected materials, a sharp fall of mechanical properties (manifesting in lower failure loads and relative elongation at rupture) was observed. Optical characteristics deteriorated as well. Application of protective coatings have been shown to reduce the degradation of mechanical and optical properties. The protection efficiency is the greatest for coatings containing silicon.

References

[1]Kleiman, J., Iskanderova, Z., Gudimenko, Y., and Horodetsky, S., "Atomic Oxygen Beam Sources: A Critical Overview," *Proceedings of 9th International Symposium on Materials in Space Environment*, ISMSE-9, European Space Research and Technology Centre, Noordwijk, The Netherlands, 2003, pp. 313–324.

[2]Rutledge, S. K., Banks, B. A., Dever, J., and Savage, W., "International Test Program for Synergistic Atomic Oxygen and VUV Exposure of Spacecraft Materials," *Proceedings of the 5th International Conference on Protection of Materials and Structures from the LEO Space Environment*, ICPMSE-5, European Space Research and Technology Centre, Arcachon, France, 2000.

[3]Akishin, A. I., Novikov, L. S., and Chernik, V. N., "Impact of Vacuum, Ionosphere Plasma Particles and Solar Ultra-Violet Radiation on Materials and Elements of Spacecraft Equipment," *New High Technologies in Techniques*, edited by L. S. Novikov and M. I. Panasyuk, Vol. 17, ENTSITEH, Moscow, 2000, pp. 100–138 (in Russian).

[4]Chernik, V. N., "Atomic Oxygen Simulation by Plasmadynamic Accelerator with Charge Exchange," *Proceedings of the 7th International*

Symposium on Materials in Space Environment, ISMSE-7, SP-399, European Space Research and Technology Centre, Toulouse, France, 1997, pp. 237–241.

[5]Rutledge, S. K., Banks, B. A., and Kitral, M., "A Comparison of Space and Ground Based Facility Environmental Effects for FEEP Teflon," NASA TM-207918/REV1, July 1998.

[6]Banks, B. A., Miller, S. K., and de Groh, K. K., "Low Earth Orbital Atomic Oxygen Interactions with Materials," NASA TM-213223, Aug. 2004.

[7]Troya, D., and Schatz, G. C., "Hypertermal Chemistry in the Gas and on Surfaces: Theoretical Studies," *International Reviews in Physical Chemistry*, Vol. 23, No. 3, 2004, pp. 341–373.

[8]Vered, R., Lempert, G. D., Grossman, E., Haruvy, Y., Marom, G., Singer, L., and Lifshitz, Y., "Atomic Oxygen Erosion on Teflon FEP and Kapton H by Oxygen from Different Sources: Atomic Force Microscopy and Complementary Studies," *Proceedings of the 6th International Symposium on Materials in Space Environment*, ISMSE-6, European Space Research and Technology Centre, Noordwijk, The Netherlands, 1994, pp. 175–179.

[9]Krech, R. H., et al., "AO Experiments at PSI," Physical Sciences, Inc., Rept. VG-96-054, Andover, MA, 1996.

[10]Paillous, A., and Pailler, C., "Behaviour of Carbon/Epoxy Composites in Simulated LEO and GEO Environments," *Proceedings of the 6th International Symposium on Materials in Space Environment*, ISMSE-6, European Space Research and Technology Centre, Noordwijk, The Netherlands, 1994, pp. 95–102.

[11]Silverman, E. M., "Space Environmental Effects on Spacecraft: LEO Materials Selection Guide," NASA CR-4661, Aug. 1995.

[12]Novikov, L. S., Chernik, V. N., Babaevskij, P. G., Kozlov, N. A., Chalyh, A. E., Balashova, E. V., and Smirnova, T. N., "Study of Black Reinforced Plastics KMU-4L with EKOM-1 Coating at Laboratory Imitation of Long Flight in Ionosphere," *Journal of Advanced Materials*, Vol. 8, No. 5, 2001, pp. 20–26.

[13]Chernik, V., Naumov, S., Demidov, S., Sokolova, S., and Svechkin, V., "Atomic Oxygen Ground and Mir Flight Testing of Polyimide Films with Various Protecting Coatings," *Proceedings of the 5th International Conference on Protection of Materials and Structures from the LEO Space Environment*, ICPMSE-5, European Space Research and Technology Centre, Arcachon, France, 2000.

[14]Chernik, V. N., Naumov, S. F., Sokolova, S. P., Gerasimova, T. I., Kurilyonok, A. O., Poruchikova, Y. V., and Novikova, V. A., "Color Polymeric Paints Research Under Atomic Oxygen in Flight and Ground-Based Experiments," *Proceedings of the 9th International Symposium on Materials in Space Environment*, ISMSE-9, European Space Research and Technology Centre, Noordwijk, The Netherlands, 2003, pp. 281–285.

J. Kleiman
Guest Editor